A Scale Space Method for Volume Preserving Image Registration

Eldad Haber[1] and Jan Modersitzki[2]

[1] Dept. of Mathematics and Computer Science, Emory University, Atlanta GA
30322, haber@mathcs.emory.edu
[2] Inst. of Mathematics, University of Lübeck, Germany
modersitzki@math.uni-luebeck.de[⋆]

Abstract. Image registration is an inherently ill-posed problem. Therefore one typically aims to provide as much information about the underlying application as possible. In particular for tumor monitoring, volume preservation of the wanted deformation is a central point. Based on [1], we propose a new scale space approach to volume preserving image registration. The main advantage of the new approach is that the constraints appear linearly and therefore the system matrices resembles Stokes matrices, which appears in computational fluid dynamics.
We present the scale space framework, a composition based numerical approach and its implementation. Finally, we demonstrate the outstanding features of this idea by a real life example.

1 Introduction

Image registration is one of the fundamental tasks in today's image processing and in particular in medical imaging; see, e.g., [2–4] and references therein. The objective of image registration is to make images which are taken at different times, from different perspectives, and/or from different devices to be more alike. Loosely, the goal of image registration is to find a "*reasonable*" deformation such that the "*distance*" between a reference image R and a deformed version of a template image T becomes small.

Image registration is an ill-posed problem (cf., e.g., [5]) and therefore need to be regularized. Different types of regularizers can be used to specify the meaning of reasonable. However, for particular applications, one may want to provide additional information. Typical examples include the knowledge of the location of anatomical landmarks or markers in the images and/or additional physical properties of the deformation field.

A situation of particular clinical interest is the analysis of pairs of images acquired before and after contrast administration; see, e.g., [6] and references therein. As a typical example, Figure 1 shows two different magnetic resonance images (MRIs) of a female breast as they are used routinely for tumor monitoring

(images from Bruce Daniel, Lucas Center for Magnetic Resonance Spectroscopy and Imaging, Stanford University). The first image shows an MRI section taken during the so-called wash-in phase of a radiopaque marker and the second image shows the analogous section during the so-called wash-out phase. A comparison of these two images indicates a suspicious region in the upper part of the images. This region can be detected easily if the images have been registered: tissue located at a certain position in the wash-in image is related to the tissue at the same position in the wash-out phase. Generally, however, a quantitative analysis is a delicate matter since observable differences are not only related to contrast uptake but also due to motion of the patient, like, for example, breathing or heart beat. Therefore, image registration becomes an inevitable task. However, as pointed out by Rohlfing et al. [6], there is a substantial difficulty with the registration of pre- and post-contrast images. Bright regions seem to enlarge during the so-called wash-in phase. This enhancement is due to contrast uptake but not to movement of the patient. Therefore, the geometry of these regions should not be changed by the registration procedure. Most importantly, for this particular application, a distance minimizing registration can produce unrealistic results. A critical feature of the wanted deformation is that it has to preserve tissue volume, particularly the tumor volume. From a clinical point of view, a volume change is unacceptable even if it results in a much smaller image distance.
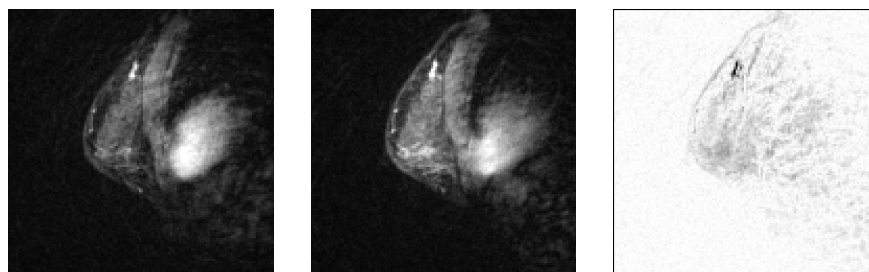
Fig. 1. MRI's of a female breast, LEFT: during the wash-in phase, MIDDLE: during the wash-out phase, and RIGHT: difference image.

A general approach to constrained image registration has been proposed in [7]. Focussing on volume preserving registration, a variational approach with a Tikhonov-type regularization has been presented. The approach leads to a nonlinear constrained optimization problem which is solved by a Sequential Quadratic Programming (SQP). At each iteration a large system of linear equations has to be solved and the iteration matrix changes as the iteration proceeds. As it is typical for constrained optimization, the system is a so-called KKT system, where for this application the off-diagonal blocks are nonlinear. In this paper, we explore a scale space type regularization applied to the constrained problem. We replace the Tikhonov regularization by a dynamical process. The regularization of the problem is obtained by performing a finite number of steps

of the discretized process. We demonstrate that this approach has unique properties when applied to the problem of volume preserving image registration. A major advantage of this new scale space approach is that the linear systems to be solved at each iteration simplify. Particularly, the off-diagonals become linear. Therefore, one can use a wealth of efficient algorithms developed for computational fluid dynamics.

This paper is organized as follows. In Section 2 we discuss the scale space regularization and formulate the system of equations it leads to. In Section 3 we discuss discretization issues of the problem. In Section 4 we present a numerical scheme for the solution of the discrete scale space problem. In Section 5 we apply the new approach and demonstrate the effectiveness of our algorithm on a realistic example.

2 Scale Space Regularization for Image Registration

In the first part we explain our notation and a straightforward Tikhonov regularization. We introduce the building blocks of our implementation. Here, for ease of presentation, we focus on the sum of squared differences (or L_2 Norm) as a distance measure (or misfit) and the elastic potential as a regularizer (or displacement semi-norm). However, other distance measures or regularizer can be used as well; see [1, 8].

In the second part we discuss our scale space Tikhonov regularization. The main observation is that a composition type approach for the transformation does allow for locally linear constraints. Therefore, a numerical treatment of the scale space approach has severe advantages.

2.1 General notations and Tikhonov regularization

With $d \in \mathbb{N}$ we denote the spatial dimension of the given images $R, T : \mathbb{R}^d \to \mathbb{R}$ which are assumed to be sufficiently smooth. Thus, $T(\boldsymbol{x})$ gives a gray value at a spatial position $\boldsymbol{x}$. Without loss of generality, we assume that the supports of the images are contained in a bounded domain $\Omega := (0, 1)^d$ and in particular $R(\boldsymbol{x}) = T(\boldsymbol{x}) = 0$ for $\boldsymbol{x} \notin \Omega$.

Our goal is to find a *"reasonable"* transformation $\boldsymbol{\varphi}$ such that the *"distance"* between the reference image and the deformed template image is small. As usual in image registration, we set $\boldsymbol{\varphi}(\boldsymbol{x}) = \boldsymbol{x} + \boldsymbol{u}(\boldsymbol{x})$ and work the displacement $\boldsymbol{u} = (u^1, \ldots, u^d)^T : \mathbb{R}^d \to \mathbb{R}^d$ rather than the transformation $\boldsymbol{\varphi}$. However, we will also use $\boldsymbol{\varphi}$ whenever it makes notation shorter.

It is well-known that the registration problem is ill-posed and therefore needs to be regularized [5]. Tikhonov-type regularization is commonly used to balance between image distance and regularity of $\boldsymbol{u}$. A mathematical formulation of the regularized and constrained problem thus reads:

$$\text{minimize} \ \ \mathcal{D}(T, R; \boldsymbol{u}) + \tfrac{\alpha}{2} \|\mathcal{B}\boldsymbol{u}\|^2 \tag{1a}$$

$$\text{subject to} \ \ \mathcal{C}(\boldsymbol{u}) = 0, \tag{1b}$$

where $\mathcal{D}$ measures image distance, $\|\mathcal{B}\boldsymbol{u}\|^2$ is a quadratic regularizer, $\mathcal{B}$ a partial differential operator, $\alpha > 0$ is a regularization parameter that compromises between similarity and regularity, and $\mathcal{C}$ are the volume preserving constraints. Problem (1) is usually solved for a sequence of decreasing α's. For each α of this sequence, we obtain a smaller misfit and a generally larger displacement semi-norm.

For ease of presentation, we focus on the Sum of Square Differences (SSD) as a distance measure,

$$\mathcal{D}(\boldsymbol{u}) := \mathcal{D}(T, R; \boldsymbol{u}) := \tfrac{1}{2}\|T(\boldsymbol{x} + \boldsymbol{u}) - R\|^2, \tag{2}$$

and the elastic potential with Lamé constants λ and μ as regularizer. Hence,

$$\mathcal{S}[\boldsymbol{u}] = \int_\Omega \langle \mathcal{B}\boldsymbol{u}, \mathcal{B}\boldsymbol{u} \rangle \ d\boldsymbol{x} \tag{3}$$

$$:= \int_\Omega \frac{\lambda + \mu}{2} \| \nabla \cdot \boldsymbol{u} \|^2 + \frac{\mu}{2} \sum_{i=1}^d \| \nabla \boldsymbol{u}_i \|^2 \ d\boldsymbol{x}.$$

For the purpose of this paper, a transformation is volume preserving if

$$\det(\nabla \boldsymbol{\varphi}(\boldsymbol{x})) = 1 \quad \text{for all} \quad \boldsymbol{x} \in \Omega;$$

see [1] for an extended discussion. Our definition implies that volume preserving maps also preserve orientation, which is an additional desirable feature in medical registration. With $I_d \in \mathbb{R}^{d,d}$ denoting the d-by-d identity matrix, our pointwise constraint thus becomes

$$\mathcal{C}(\boldsymbol{u}) := \det(I_d + \nabla \boldsymbol{u}) - 1 = 0. \tag{4}$$

Introducing a Lagrange multiplier p, the Lagrangian of (1) is

$$\mathcal{L}(\boldsymbol{u}, p) = \tfrac{1}{2}\|T(\boldsymbol{u}) - R\|^2 + \frac{\alpha}{2}\|\mathcal{B}\boldsymbol{u}\|^2 + \int_\Omega \mathcal{C}(\boldsymbol{u}) \cdot p \ d\boldsymbol{x}$$

and the continuous Euler-Lagrange equations for (1) are

$$0 = (\nabla T(\boldsymbol{u}))^\top (T(\boldsymbol{u}) - R) + \alpha \mathcal{B}^* \mathcal{B}\boldsymbol{u}$$
$$\qquad - \nabla \cdot [\det(I_d + \nabla \boldsymbol{u})(I_d + \nabla \boldsymbol{u})^{-\top} \cdot p], \tag{5a}$$
$$0 = \det(I_d + \nabla \boldsymbol{u}) - 1, \tag{5b}$$
$$0 = \boldsymbol{n} \cdot \nabla \boldsymbol{u}_i; \quad i = 1..d \tag{5c}$$

see [7]. Here, ∇T is the gradient of T and $\mathcal{B}^*$ the adjoint of $\mathcal{B}$. The system (5) is a highly coupled system of nonlinear partial differential equations (PDE). The differential operator $\mathcal{B}^*\mathcal{B}$ in (5a) is a linear, elliptic operator. The last term in (5a) is related to the derivative of the constraints which also show up in (5b). It is not easy to show either existence or uniqueness of a solution of the PDE (5).

For the purpose of this paper, we therefore assume existence of a solution and remark that proving its existence is a subject of further research.

After freezing the coefficients of the linearized system (5), a Local Fourier Analysis can be used to show ellipticity of the system for small displacements $\boldsymbol{u}$; see, e.g. [9]. However, for large displacements ellipticity is crucial and numerical difficulties may arise; see [1]. This motivates us to use a modified Iterative Tikhonov Regularization approach where only small displacements are considered and a sequence of elliptic problems has to be solved.

2.2 A Modified Iterated Tikhonov regularization

We now explore a modified iterated Tikhonov regularization approach and show that it has some favorable numerical properties.

We assume that at some stage k we have an approximate solution $\boldsymbol{\varphi}_k(\boldsymbol{x}) = \boldsymbol{x} + \boldsymbol{u}_k(\boldsymbol{x})$ which is volume preserving and therefore obeys Eq. (4). We can also associate to this solution an image distance $\mathcal{D}(\boldsymbol{u}_k)$ and a displacement norm $\|\mathcal{B}\boldsymbol{u}_k\|^2$. We seek a method to update $\boldsymbol{\varphi}_k$ such that the new transformation $\boldsymbol{\varphi}_{k+1}$ gives a smaller image distance and an equal or larger displacement norm. Using the common iterated Tikhonov regularization techniques, one would compute a linear perturbation $\boldsymbol{v}$ and set

$$\boldsymbol{\varphi}_{k+1} = \boldsymbol{\varphi}_k + \boldsymbol{v}_k \quad \text{or} \quad \boldsymbol{u}_{k+1} = \boldsymbol{u}_k + \boldsymbol{v}_k. \tag{6}$$

However, this straightforward approach does not lead to a simplification of the equations or to an improvement of the numerics. The main problem is that the volume preserving constraint is nonlinear and therefore

$$\mathcal{C}(\boldsymbol{u}_k + \boldsymbol{v}_k) \neq \mathcal{C}(\boldsymbol{u}_k) + \mathcal{C}(\boldsymbol{v}_k).$$

A better approach is to update the whole $\boldsymbol{\varphi}_k$ in terms of a composition. This can be done by computing a new function $\boldsymbol{\psi}_k(\boldsymbol{x}) = \boldsymbol{x} + \boldsymbol{v}_k(\boldsymbol{x})$ and setting

$$\boldsymbol{\varphi}_{k+1}(\boldsymbol{x}) = \boldsymbol{\varphi}_k(\boldsymbol{\psi}_k(\boldsymbol{x})) \quad \text{or} \quad \boldsymbol{u}_{k+1}(\boldsymbol{x}) = \boldsymbol{u}_k(\boldsymbol{x} + \boldsymbol{v}_k(\boldsymbol{x})) + \boldsymbol{v}_k(\boldsymbol{x}).$$

The following Lemma is a key observation for the development of an efficient algorithm.

Lemma 1. *The set of volume preserving mappings with the composition is a non-commutative group.*

Proof. Since the set of continuous functions forms a group with respect to composition, the statement follows from

$$\det(\nabla[\boldsymbol{\varphi}(\boldsymbol{\psi}(\boldsymbol{x}))]) = \det(\nabla\boldsymbol{\varphi}(\boldsymbol{\psi}(\boldsymbol{x})) \cdot \nabla\boldsymbol{\psi}(\boldsymbol{x})) = \det(\nabla\boldsymbol{\varphi}) \cdot \det(\nabla\boldsymbol{\psi}) = 1,$$

where $\boldsymbol{\varphi}$ and $\boldsymbol{\psi}$ are assumed to be volume preserving. ∎

The above Lemma allows us to derive efficient algorithms. At stage k, we define $T_k(\boldsymbol{x}) := T(\boldsymbol{\varphi}_k(\boldsymbol{x}))$. We are than seeking for a (small) update $\boldsymbol{v}$ as a solution of

$$\text{minimize} \quad \tfrac{1}{2}\|T_k(\boldsymbol{x}+\boldsymbol{v}) - R\|^2 + \tfrac{\alpha}{2}\|\mathcal{B}\boldsymbol{v}\|^2 \tag{7a}$$

$$\text{subject to} \quad \mathcal{C}(\boldsymbol{v}) = 0. \tag{7b}$$

Note that for a minimizer $\boldsymbol{v}_k$ of problem (7) we have

$$T_k(\boldsymbol{x}+\boldsymbol{v}_k) = T(\boldsymbol{\varphi}_k(\boldsymbol{x}+\boldsymbol{v}_k)) = T(\boldsymbol{\varphi}_k(\boldsymbol{\psi}_k(\boldsymbol{x}))).$$

In contrast to the straightforward linear approach (6), the new approach is based on composition. This approach is related to the Euler coordinates framework as used in fluid registration [10], see also [5, §10.4.2]. In other words, we change from material to spatial coordinates but drop the material derivative within the regularizer. Thus, the new scale space approach give different solutions than the Iterative Tikhonov regularization. In the next section we demonstrate that the solution of the sequence of problems (7) can be computed very effectively using a Newton-Multigrid method.

3   Discretization

There are two main approaches for the discretization of the registration problems (1) and (7)). In the first so-called *optimize-discretize* approach one forms the objective function, then differentiates to obtain the continuous Euler-Lagrange equations, which are finally discretized and solved numerically; see, e.g., [11, 12, 5]. In the second so-called *discretize-optimize* approach one directly discretizes the problem and then solves a finite but typically high-dimensional optimization problem; see, e.g., [1]. The advantage of the latter approach is that standard optimization methods can be used. We therefore prefer the discretize-optimize approach. However, in order to take advantage of efficient optimization techniques, all parts of the discrete problem need to be continuously differentiable.

Choosing a stable discretization method for a system of partial differential equations (PDE's) with mixed derivatives is a non-trivial matter. As proposed in [1], we use staggered grids (cf. Figure 2) which are very common for stable discretizations of the related problem of incompressible fluid flow (see, e.g., [13]) and electromagnetics (see, e.g., [14, 15]) where operators such as the gradient, curl, and divergence are discretized.

In this section we briefly summarize the discretization we use. Further discussion and details are given in [7].

3.1   Discretizing u and $\mathcal{S}$

We assume that our discrete images have $m_1 \times \ldots \times m_d$ pixels, where $d = 2, 3$ is the image dimensionality. For ease of presentation, we also assume that each pixel is square or cubic where each side has length h. In our description we allow for
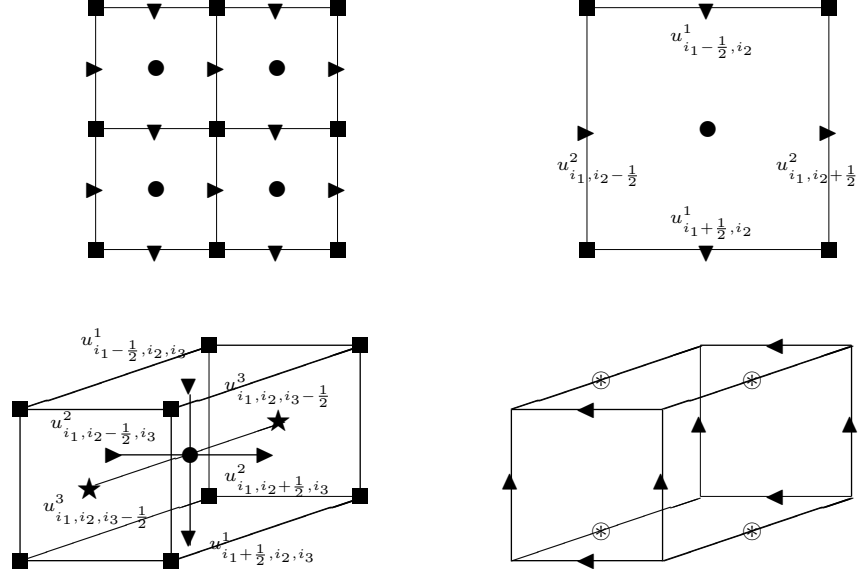
Fig. 2. Staggered grids for dimensions $d = 2, 3$, nodal ■, cell centered •, face staggered grids (▼ in x_1-, ▶ in x_2-, and ★ in x_3-direction), and edge staggered grids (▲ in x_1-, ◀ in x_2-, and ⊛ in x_3-direction). TOP LEFT: $d = 2$, four pixels, TOP RIGHT: $d = 2$ pixel (i_1, i_2) with grids, BOTTOM LEFT: $d = 3$, voxel (i_1, i_2, i_3) with face staggered grids and positions of u^1, u^2, u^3, BOTTOM RIGHT: $d = 3$, edge staggered grids.

half step indices. As usual in image processing, we identify pixels/voxels with cell centered grid points $x_{j,k,\ell}$, which are therefore labeled with full integers indices. Given a pixel/voxel $x_{j,k,\ell}$, their faces are numbered with a half index, $x_{j\pm\frac{1}{2},k,\ell}$, $x_{j,k\pm\frac{1}{2},\ell}$, and $x_{j,k,\ell\pm\frac{1}{2}}$, and we discretize the ith component u^i of $\boldsymbol{u}$ on the ith face for every pixel/voxel. With some abuse of notation, we denote the discrete analog of the continuous vector field by $\boldsymbol{u} = (u^1, \ldots, u^d)^\top$, where u^i denotes the grid function which is approximated on the face-staggered grid.

If needed, the derivatives $\partial_j u^k$ are approximated by the short (central) differences,

$$\partial_j u^k \approx \partial_j^h u^k := \tfrac{1}{h}(u^k_{\ldots,i_j+\frac{1}{2},\ldots} - u^k_{\ldots,i_j-\frac{1}{2},\ldots}). \tag{8}$$

Note that no boundary conditions are needed to approximate derivatives in the normal directions ($\partial_j u^j$). For the tangential directions ($\partial_j u^k$, $j \neq k$) we imposed Neumann boundary conditions.

Since many regularizers are phrased in terms of the more complex differential operators ∇ and divergence $\nabla\cdot$, we introduce the notation ∇^h and $\nabla^h\cdot$ for the discrete analogs. Using these discrete analogs the elastic potential $\mathcal{S}$ is discretized

as

$$\|\boldsymbol{Bu}\|^2 := \frac{\lambda + \mu}{2} \| \nabla^h \cdot \boldsymbol{u}\|^2 + \frac{\mu}{2} \sum_{i=1}^{d} \| \nabla^h \boldsymbol{u}_i\|^2$$

In the course of the registration process we require derivatives. Upon differentiation of the regularizer we obtain the Navier-Lamé operator

$$\frac{1}{2} \frac{\partial \|\boldsymbol{Bu}\|^2}{\partial \boldsymbol{u}} = (\lambda + \mu)(\nabla^h \cdot)^{\top} \nabla^h \cdot \boldsymbol{u} + \mu \Delta^h \boldsymbol{u} =: \boldsymbol{Au}.$$

where Δ^h is the vector Laplacian on a staggered grid

3.2 Discretizing T and $\mathcal{D}$

We are heading for fast and efficient optimization scheme and therefore differentiability does play a key role. Thus, although computationally superior, d-linear image approximations can not be used, since they are not continuously differentiable.

If we require a continuously differentiable objective function we require to have a continuous image model. Since the images are typically noisy but derivatives are needed we use a smoothing B-spline to approximate the image where the smoothing parameter is chosen using the Generalized Cross Validation method [16]. For data interpolation using B-splines see [17]. Since the grid is regular, we can quickly evaluate the spline coefficients using a cosine transform. The continuous smooth approximation is denoted by T^{spline}; see [1] for details.

Given the staggered grid representation of $\boldsymbol{u}$ we use averaging operators P_j for the transfer to the cell centered positions, we set

$$T(\boldsymbol{u}) := T^{\mathrm{spline}}(x^1 + P_1 u^1, \ldots, x^d + P_d u^d),$$

see [7] for details. We denote the Jacobian of T by

$$T_{\boldsymbol{u}} := \frac{\partial T}{\partial \boldsymbol{u}}(\boldsymbol{u}) = \Big(\mathrm{diag}(P_1^{\top} \partial_1 T), \ldots \mathrm{diag}(P_d^{\top} \partial_d T)\Big),$$

where the partial derivatives $\partial_j T$ are evaluated at the spatial positions $(x^1 + P_1 u^1, \ldots, x^d + P_d u^d)$. Using a spline approximation for T, $T_{\boldsymbol{u}}$ becomes a sparse matrix with only four non-zero diagonals.

Our discretization of the SSD (2) is straightforward,

$$\boldsymbol{D}(\boldsymbol{u}) := \tfrac{1}{2}\|T(\boldsymbol{u}) - R\|_2^2 \quad \text{and thus} \quad \boldsymbol{D}_{\boldsymbol{u}}(\boldsymbol{u}) = T_{\boldsymbol{u}}(\boldsymbol{u})^{\top}(T(\boldsymbol{u}) - R).$$

3.3 Discretizing $\mathcal{C}$

In our discretization of the volume preserving constraints we note that derivatives of every field to every direction are needed and that they need to be centered at the same location. We shortly review the work in [7]. To simplify the discussion we discuss the 2D case only, the extension to 3D is lengthy but straightforward.

In 2D the constraint reads

$$\mathcal{C}(\boldsymbol{u}) = \nabla \cdot \boldsymbol{u} + u_x^1 u_y^2 - u_y^1 u_x^2 = u_x^1 + u_y^2 + u_x^1 u_y^2 - u_y^1 u_x^2.$$

Using the short difference (8) the derivatives u_x^1 and u_y^2 naturally centered at the cell center. To discretize derivatives in the tangential direction we simply use long differences.

4 The discrete scale space process

After discretization we obtain a discrete scale space process. At each iteration we require to approximately solve the discrete system

$$\text{minimize} \quad \tfrac{1}{2}\|T_k(\boldsymbol{v}) - R\|^2 + \tfrac{\alpha}{2}\|\boldsymbol{B}\boldsymbol{v}\|^2 \tag{9a}$$

$$\text{subject to} \quad \boldsymbol{C}(\boldsymbol{v}) = 0. \tag{9b}$$

Common to other iterative regularization methods (cf., e.g., [18]), we use a single Gauss-Newton step to approximate the solution of the discrete system (9) and immediately update T_k. After linearization we obtained the following quadratic constrained optimization problem

$$\text{minimize} \quad \tfrac{1}{2}\|T_k + (\nabla^h T_k)\boldsymbol{v} - R\|^2 + \tfrac{\alpha}{2}\|\boldsymbol{B}\boldsymbol{v}\|^2$$

$$\text{subject to} \quad \nabla^h \cdot \boldsymbol{v} = 0.$$

The main advantage of the scale space approach is that the constraints in (9) are linearized with respect to $\boldsymbol{v}$. Therefore, the nonlinear parts vanish and we end up with linear constraints. The Gauss-Newton step is given by the solution of

$$\begin{pmatrix} \boldsymbol{M} + \alpha\boldsymbol{A} & (\nabla^h \cdot)^\top \\ \nabla^h \cdot & \boldsymbol{0} \end{pmatrix} \begin{pmatrix} \boldsymbol{v} \\ \boldsymbol{p} \end{pmatrix} = \begin{pmatrix} (\nabla^h T_k)^\top (T_k - R) \\ \boldsymbol{0} \end{pmatrix}, \tag{10}$$

where $\boldsymbol{p}$ is a discrete Lagrange multiplier and $\boldsymbol{M}$ is a diagonal positive semi-definite matrix which approximates $(\nabla^h T_k)^\top \nabla^h T_k$. The system (10) is similar to the Stokes system in Fluid Dynamics. It is well known that staggered discretization is crucial in order to obtain a stable system; see, e.g., [13]. For Fluid Dynamic problems, effective numerical methods where developed; see, e.g., [19, 20]). In particular, multigrid solvers are among the most efficient schemes to solve problem (10).

The system (10) is solved numerically and $\boldsymbol{v}$ is updated. However, since $\boldsymbol{v}$ is a solution for the linearized problem, this update may not be volume preserving. In order to guarantee the volume preservation of our numerical solution, we explicitly project this solution onto the constraint. As explained in [1], the projection is computed by solving

$$\boldsymbol{C}(\boldsymbol{v} + \boldsymbol{w}) = 0$$

for the correction $\boldsymbol{w}$. To be precise, we compute a least squares solution of the linearized problem

$$\boldsymbol{C}(\boldsymbol{v} + \boldsymbol{w}) \approx \boldsymbol{C}(\boldsymbol{v}) + \boldsymbol{C}_{\boldsymbol{v}}\boldsymbol{w} = 0, \tag{11}$$

where C_v is the derivative of C. This system is underdetermined because we have less equations than unknowns. The above process can be thought of as an orthogonal projection to the volume preserving constraint.

The above algorithm is summarized in Algorithm 1.

Algorithm 1
A scale space approach to volume preserving image registration.
$u \leftarrow \mathrm{SPIR}(\alpha, u)$;

---

  set $k = 0$, $T_k(x) = T(x)$, $\varphi_k(x) = x$;
  while not stop **do**
    compute image distance, displacement semi-norm, and M;
    set up system (10) and solve for v;
    project to the constraint by solving (11) for w;
    set $\psi_k(x) = x + v + w$ and $\varphi_{k+1}(x) = \varphi_k(\psi_k(x))$;
    compute $T_{k+1}(x) = T(\varphi_{k+1}(x))$;
    update $k \leftarrow k + 1$;
  end while

---

5   A numerical example and discussion

To demonstrate the effectiveness of our new scale space approach we apply the algorithm to the breast images in Figure 1. The images where analyzed in [7] using the straighforward Tikhonov regularization discussed in Section 2.1 and we use them for comparison here. The magnetic resonance images are noisy and only slightly shifted and therefore it is expected that a small number of scale space iterations is needed to achieve a sufficient level of image similarity. Indeed, setting the regularization parameter of each iteration to $\alpha = 10^{-4}$ it takes nine iterations to obtain a relative image distance of 0.87. The history of the iteration is presented in Table 1.

The Tikhonov regularization approach presented in [7] takes ten iterations with a fixed regularization parameter $\alpha = 10^{-5}$ to achieve about the same image distance and about the same displacement semi-norm. For this particular example, the images and the displacements obtained using the new scale space approach and those obtained from the Tikhonov regularization method are visually identical; see Figure 3.

Table 1. The relative image distance $D(u_k)/D(0)$ and the displacement semi-norm versus iteration k for the scale space iteration.

iteration	1	2	3	4	5	6	7	8	9
distance	0.98	0.96	0.91	0.90	0.90	0.89	0.88	0.88	0.87
$10^3 \cdot \|Bu\|^2$	1.2	1.4	1.8	1.7	1.8	1.8	1.9	2.0	2.0
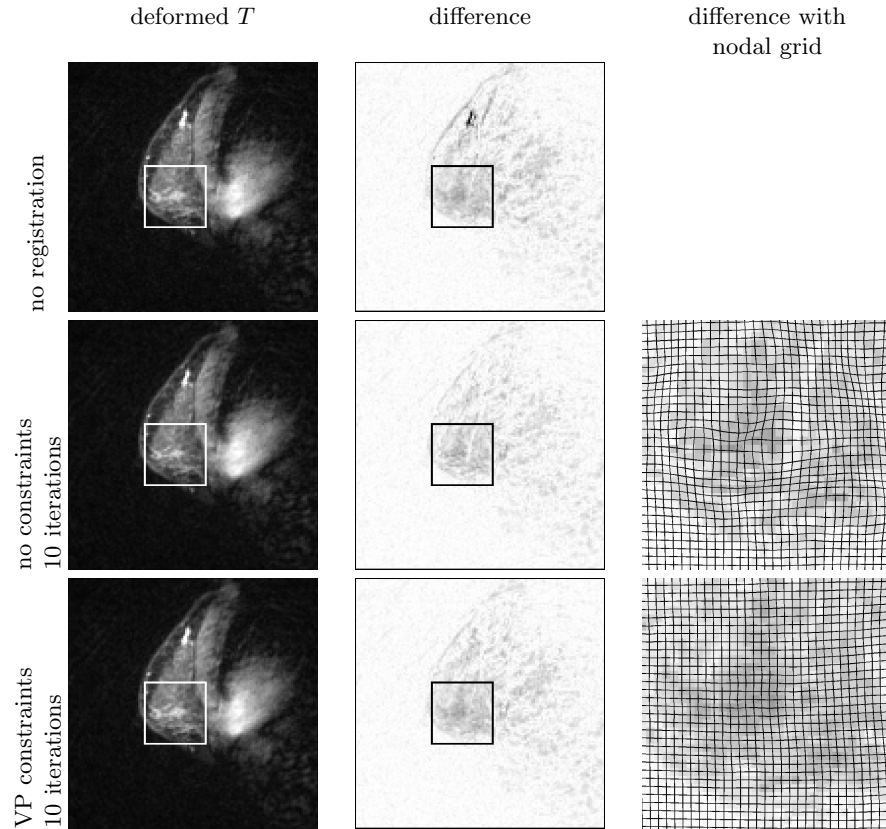
Fig. 3. Registration results for the images of Fig. 1. LEFT COLUMN deformed template images T_k, MIDDLE COLUMN difference image $|R-T_k|$ with a region of interest (ROI), RIGHT COLUMN ROI with nodal grid, vertices connected by straight lines ; ROW 1: no registration, ROW 2: no constraints ten iterations, and ROW 3: volume preserving constraints ten iterations.

There are two main advantages to the scale approach over the Traditional Tikhonov regularization. First, every iteration of the scale space method is significatively simpler compared with the Tikhonov regularization approach. The main advantage is that the iteration matrix is fixed and therefore efficient methods can be designed for the solution of the linear system. In particular, the system is similar to the Stokes system and we intend to explore the use of multigrid methods for its solution in a consecutive paper. The second advantage is that we need not search for the regularization parameter. A rough choice is sufficient and the SSD is reduced by the scale space iteration.

References

1. Haber, E., Modersitzki, J.: Numerical methods for volume preserving image registration. Inverse Problems, Institute of Physics Publishing **20** (2004) 1621–1638
2. Maurer, C.R., Fitzpatrick, J.M.: A Review of Medical Image Registration. In: Interactive Image-Guided Neurosurgery. Park Ridge, IL, American Association of Neurological Surgeons (1993) 17–44
3. Fitzpatrick, J.M., Hill, D.L.G., Jr., C.R.M.: Image registration, handbook of medical imaging. Volume 2: Medical Image Processing and Analysis, SPIE (2000) 447–513
4. Zitová, B., Flusser, J.: Image registration methods: a survey. Image and Vision Computing **21** (2003) 977–1000
5. Modersitzki, J.: Numerical methods for image registration. Oxford (2004)
6. Torsten Rohlfing, Calvin R. Maurer, J.D.A.B., Jacobs, M.A.: Volume-preserving nonrigid registration of MR breast images using free-form deformation with an incompressibility constraint. IEEE Transactions on Medical Imaging **22** (2003) 730–741
7. Haber, E., Modersitzki, J.: Numerical solutions of volume preserving image registration. Inverse Problems **20** (2004) 1621–1638
8. Fischer, B., Modersitzki, J.: A unified approach to fast image registration and a new curvature based registration technique. Linear Algebra and its Applications **380** (2004) 107–124
9. Trottenberg, U., Oosterlee, C., Schüller, A.: Multigrid. Academic Press (2001)
10. Christensen, G.E.: Deformable shape models for anatomy. PhD thesis, Sever Institute of Technology, Washington University (1994)
11. Henn, S., Witsch, K.: Iterative multigrid regularization techniques for image matching. SIAM J. on Scientific Comp. (2001) 1077–1093
12. Clarenz, U., Droske, M., Rumpf, M.: Towards fast non–rigid registration. In: Inverse Problems, Image Analysis and Medical Imaging, AMS Special Session Interaction of Inverse Problems and Image Analysis. Volume 313., AMS (2002) 67–84
13. Fletcher, C.: Computational Techniques for Fluid Dynamics. Volume II. Springer-Verlag (1988)
14. Yee, K.: Numerical solution of initial boundary value problems involving Maxwell's equations in isotropic media. IEEE Trans. on antennas and propagation **14** (1966) 302–307
15. Haber, E., Ascher, U.: Fast finite volume simulation of 3D electromagnetic problems with highly discontinuous coefficients. SIAM J. Scient. Comput. **22** (2001) 1943–1961
16. Golub, G., Heath, M., Wahba, G.: Generalized cross-validation as a method for choosing a good ridge parameter. Technometrics **21** (1979) 215–223
17. Wahba, G.: Spline Models for Observational Data. SIAM, Philadelphia (1990)
18. Engl, H., Hanke, M., Neubauer, A.: Regularization of Inverse Problems. Kluwer (1996)
19. Silvester, D., Elman, H., Kay, D., Wathen, A.: Efficient preconditioning of the linearized Navier-Stokes equations. J. Comp. Appl. Math. **128** (2001) 261–279
20. Trottenberg, U., Oosterlee, C., Schuller, A.: Multigrid. Academic Press (2001)